Cell Reports
Article

Gli Protein Activity Is Controlled by Multisite Phosphorylation in Vertebrate Hedgehog Signaling

Pawel Niewiadomski,[1,2,5,*] Jennifer H. Kong,[4,7] Robert Ahrends,[3,6,7] Yan Ma,[1,2] Eric W. Humke,[1,2,8] Sohini Khan,[1,2] Mary N. Teruel,[3] Bennett G. Novitch,[4] and Rajat Rohatgi[1,2,*]

[1]Department of Medicine, Stanford University School of Medicine, Stanford, CA 94305, USA
[2]Department of Biochemistry, Stanford University School of Medicine, Stanford, CA 94305, USA
[3]Department of Chemical and Systems Biology, Stanford University School of Medicine, Stanford, CA 94305, USA
[4]Department of Neurobiology, Eli and Edythe Broad Stem Cell Research Center, David Geffen School of Medicine at UCLA, Los Angeles, CA 90095, USA
[5]Department of Cell Biology, Nencki Institute of Experimental Biology, 02-093 Warsaw, Poland
[6]Laboratory of Quantitative Systems Analysis, Leibniz-Institute for Analytical Sciences (ISAS) e.V., 44227 Dortmund, Germany
[7]These authors contributed equally to this work
[8]Present address: Genentech, Inc., Early Clinical Development, 1 DNA Way, M/S 442, South San Francisco, CA 94080, USA
*Correspondence: p.niewiadomski@nencki.gov.pl (P.N.), rrohatgi@stanford.edu (R.R.)
http://dx.doi.org/10.1016/j.celrep.2013.12.003

SUMMARY

Gli proteins are transcriptional effectors of the Hedgehog (Hh) pathway in both normal development and cancer. We describe a program of multisite phosphorylation that regulates the conversion of Gli proteins into transcriptional activators. In the absence of Hh ligands, Gli activity is restrained by the direct phosphorylation of six conserved serine residues by protein kinase A (PKA), a master negative regulator of the Hh pathway. Activation of signaling leads to a global remodeling of the Gli phosphorylation landscape: the PKA target sites become dephosphorylated, while a second cluster of sites undergoes phosphorylation. The pattern of Gli phosphorylation can regulate Gli transcriptional activity in a graded fashion, suggesting a phosphorylation-based mechanism for how a gradient of Hh signaling in a morphogenetic field can be converted into a gradient of transcriptional activity.

INTRODUCTION

The Hedgehog (Hh) pathway is an evolutionarily conserved signaling system that plays a central role in embryogenesis and adult tissue homeostasis. Its misregulation leads to developmental defects and to cancers of the skin and the brain (Briscoe and Thérond, 2013; Hahn et al., 1996). The Gli (*Gli*oblastoma) transcription factors in vertebrates control the Hh gene expression program (Hui and Angers, 2011). Despite the importance of Gli proteins in development, regeneration, and cancer, the mechanism by which they acquire the ability to activate target genes has remained enigmatic.

Among the three mammalian Gli proteins, Gli2 and Gli3 are the first responders to the Hh signal. Once activated, Gli2/3 then induce the expression of Gli1, which acts as an amplifier of the response. Gli2/3 can perform two opposing functions at target promoters (Figure 1A; reviewed in Hui and Angers, 2011). When the pathway is off, Gli2/3 proteins are converted into truncated repressor forms (hereafter abbreviated GliR), which inhibit target gene transcription. When the Hh ligand is received, GliR production is blocked and Gli2/3 proteins are converted into transcriptional activators (hereafter abbreviated GliA). In the nucleus, the balance between GliR and GliA shapes the Hh response. Between these two extremes, a substantial fraction of Gli2/3 remains in the cytoplasm in a transcriptionally inactive state (Humke et al., 2010). Quantitative changes in the GliR/GliA ratio can lead to developmental defects in humans, underscoring the point that the precise level of Gli activity is often critical for the sophisticated patterning events regulated by Hh signaling during development (Hill et al., 2007; Kang et al., 1997; Wang et al., 2000).

GliR and GliA production are both controlled by the seven-transmembrane protein Smoothened (Smo; Figure 1A). Upon Hh ligand reception by Patched (Ptc), Smo accumulates in a microtubule-based protrusion of the cell membrane known as the primary cilium (Corbit et al., 2005). Through an unknown mechanism, ciliary Smo inhibits GliR formation and induces the transport of Gli proteins to the tips of cilia (Kim et al., 2009; Wen et al., 2010), where they dissociate from the negative regulator Suppressor of Fused (SuFu; Humke et al., 2010; Tukachinsky et al., 2010). Thereupon, Glis translocate into the nucleus and activate target genes. Nuclear Gli proteins are characterized by a short half-life and reduced mobility on SDS-PAGE gels caused by a distinct phosphorylation event, hereafter referred to as "hyperphosphorylation" (Humke et al., 2010).

The mechanistic details of the interaction between Smo and Gli proteins are not understood. Several lines of evidence point to protein kinase A (PKA) as a key regulator of the Hh signal

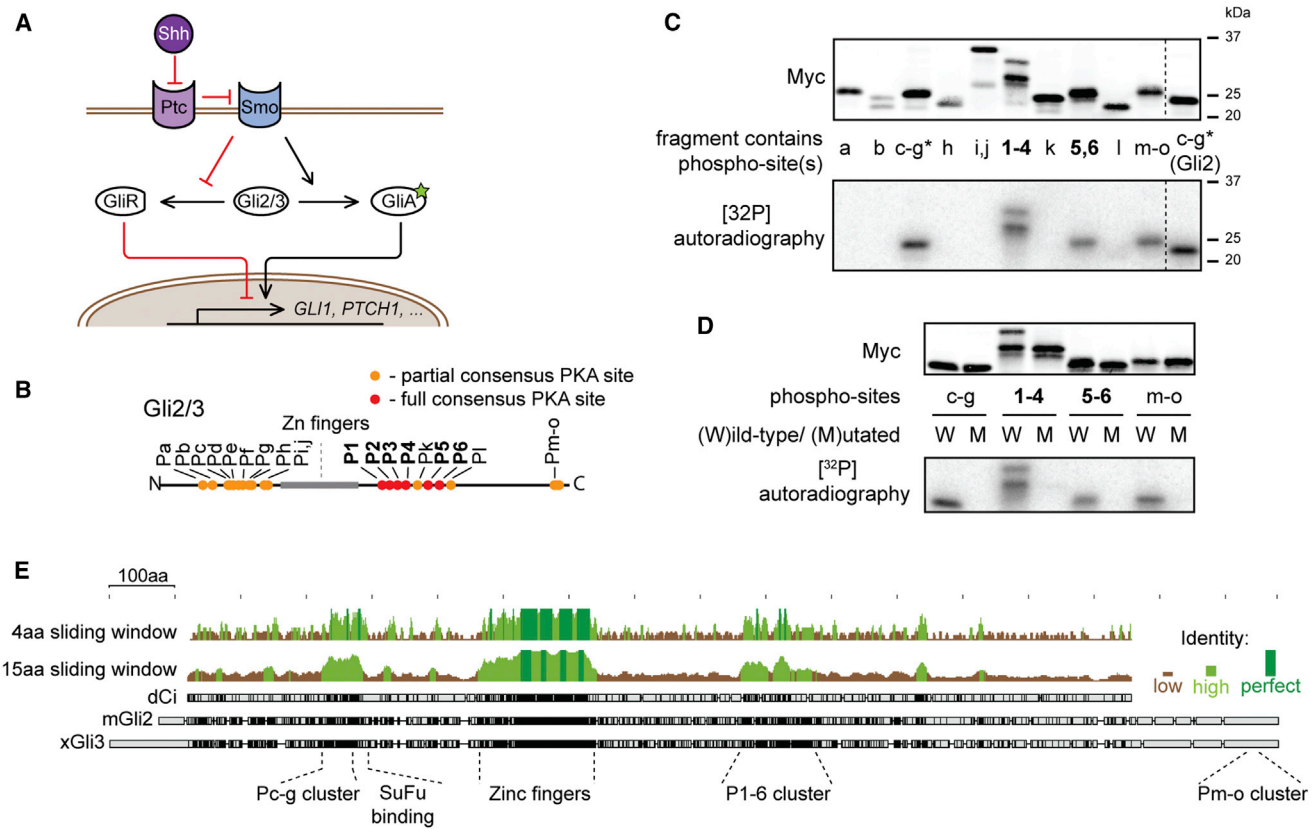

Figure 1. PKA Phosphorylates Both Full and Partial Consensus Sites on Gli2/3 In Vitro

(A) Schematic representation of Gli2/3 regulation by Hh signaling. Active Smo induces the formation of GliA and suppresses the production of the truncated GliR.

(B) Location of the full (red dots; P1–6) and partial consensus (orange dots; Pa–o) PKA target sites that are conserved in both mouse and human Gli2 and Gli3.

(C) In vitro PKA phosphorylation of Myc-tagged Gli3 fragments containing the indicated target sites. An anti-myc immunoblot (top) shows total protein levels of each fragment in the assay and the autoradiogram (bottom) shows ^{32}P incorporation. The Pc-g (*) fragment was tested for both Gli3 and Gli2 since only the former contains an additional PKA consensus target sequence.

(D) S/T residues presumed to be PKA targets were mutated in Gli3 fragments containing sites Pc-g, P1–4, P5,6, and Pm–o. Wild-type (W) or mutant (M) fragments were subjected to in vitro phosphorylation as in (C).

(E) Protein sequences of *Drosophila* Ci, mouse Gli2, and *Xenopus* Gli3 were aligned using the Geneious algorithm and the degree of conservation of protein sequences was plotted for either a 4-amino-acid or 15-amino-acid sliding window.

downstream of Smo (Fan et al., 1995; Hammerschmidt et al., 1996; Hynes et al., 1995; Jiang and Struhl, 1995; Lepage et al., 1995; Li et al., 1995; Niewiadomski et al., 2013; Pan and Rubin, 1995; Strutt et al., 1995; Tuson et al., 2011). Pharmacological activation of PKA completely blocks Hh signaling, even in the presence of the Hh ligand or a Smo agonist. Conversely, genetic ablation of PKA shifts the GliR/GliA balance strongly in favor of GliA. This leads to full ligand-independent activation of Hh target genes, manifested as complete ventralization of the embryonic neural tube in mutant mice (Tuson et al., 2011). These data clearly identify PKA as a negative regulator of Gli function, but on a molecular level, our understanding of how Gli proteins are influenced by PKA remains incomplete.

The mechanism by which PKA promotes GliR has been elucidated in detail, guided by studies of the *Drosophila* Gli homolog *cubitus interruptus* (Ci; Aza-Blanc et al., 1997; Méthot and Basler, 1999; Price and Kalderon, 1999; Wang et al., 1999). PKA can phosphorylate Gli2/3 at six conserved serine residues (P1–6) located on the carboxyterminal side of the DNA binding Zn-finger domain (Figure 1B; Wang et al., 2000). The phosphorylation of the first four of these residues (P1–4) by PKA initiates a pathway that leads to the partial processing of full-length Glis into GliR fragments by the proteasome (Pan et al., 2009; Wang et al., 1999); the function of the last two phosphorylation sites (P5,6) is unknown.

PKA plays an equally important but much less well-understood role in suppressing Gli2/3A. Loss of phosphorylation at sites P1–4, which regulates GliR production, does not seem to be sufficient for this activation step. Transgenic mice harboring nonphosphorylatable serine-to-alanine mutations in P1–4 of Gli2 do not show the developmental phenotypes expected if Gli2 was fully activated (Pan et al., 2009). Importantly, the neural tube of these animals, in contrast to animals lacking PKA activity, is not strongly ventralized. Thus, PKA must inhibit Gli2 activation by phosphorylating sites other than P1–4.

Here, we elucidate the mechanism by which PKA inhibits the production of GliA. PKA uses distinct phosphorylation patterns

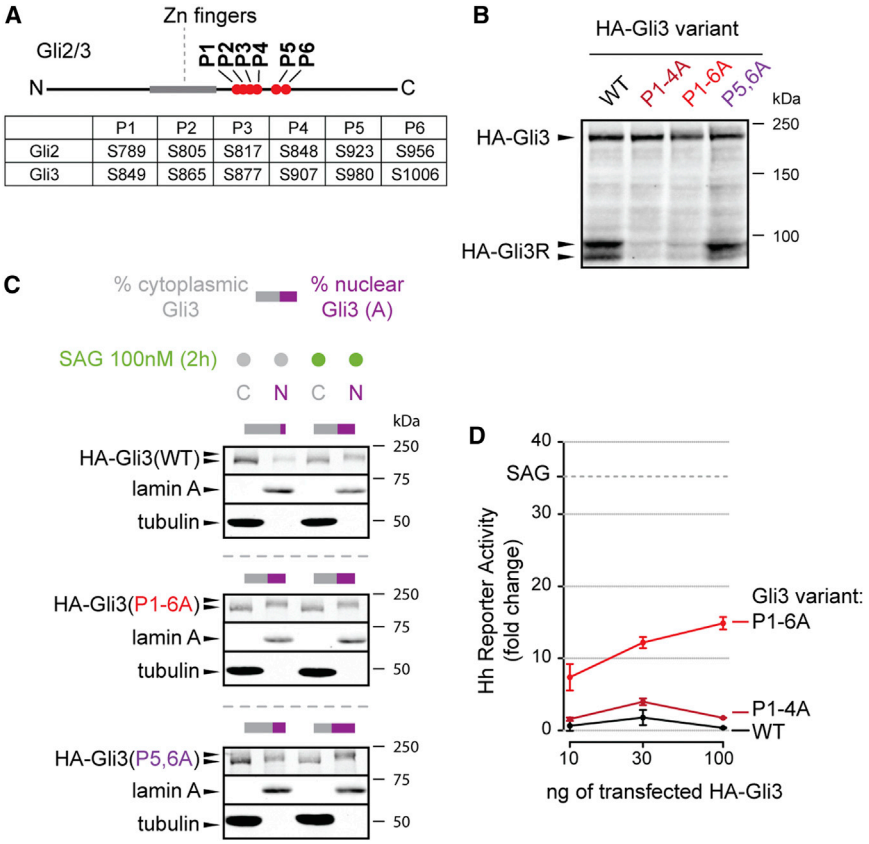

	P1	P2	P3	P4	P5	P6
Gli2	S789	S805	S817	S848	S923	S956
Gli3	S849	S865	S877	S907	S980	S1006

Figure 2. The P1–6 Cluster Regulates the Balance between Gli3 Activator and Gli3 Repressor

(A) Location of sites P1–6 on mouse Gli2 and Gli3.

(B) An anti-HA immunoblot reveals the relative levels of full-length and repressor Gli3 in whole-cell extracts from NIH/3T3 Flp-In cells stably expressing HA-tagged Gli3 variants.

(C) Distribution of full-length HA-Gli3 variants in the nuclear (N) and cytoplasmic (C) fractions of NIH/3T3 Flp-In cells left untreated or treated with SAG (100 nM, 2 hr). In this and subsequent figures, lamin A and tubulin serve as control nuclear and cytoplasmic proteins to assess the quality of the fractionation and bars above each blot represent the relative abundance of HA-Gli3 in the cytoplasmic (gray) and nuclear (purple) fractions as determined by quantitative immunoblotting. Figure S2B compiles data from five repeats of such an experiment.

(D) Activation of a luciferase-based Hh reporter gene in NIH/3T3 cells (untreated with any Hh agonists) transiently transfected with the reporter construct in combination with the indicated Gli3 variants. Values were normalized to reporter induction seen with an empty plasmid (control). Dashed gray line shows the level of reporter activation seen with SAG (100 nM; 24 hr) in cells transfected with a control vector. See also Figure S2C. Error bars indicate SD from three independent transfections.

to regulate GliR and GliA; phosphorylation of P1–4 is sufficient for GliR production, while the inhibition of GliA formation is dependent on all six sites from the P1–6 cluster. Smo activation reduces phosphorylation of P1–6, showing that Hh signaling wields direct control over phosphorylation at these sites. We also find that P1–6 *de*phosphorylation allows the phosphorylation of Gli2 at a distinct cluster of sites, which plays a positive role in Hh signaling. We propose that remodeling of the phosphorylation landscape of Gli2/3 proteins controls the transcriptional output of Hh signaling and discuss the implications of this model for the role of Hh as a morphogen in development.

RESULTS

PKA Phosphorylates Gli2/3 at Multiple Sites In Vitro

Previous work has implicated PKA both in GliR formation and in GliA inhibition (Hammerschmidt et al., 1996; Pan et al., 2009; Tuson et al., 2011; Wang et al., 1999, 2000), but the biochemical mechanism by which PKA blocks GliA formation was unknown. We hypothesized that PKA suppresses the formation of GliA by direct phosphorylation of Gli2/3. In order to identify putative inhibitory PKA target sites on Gli2/3, we looked for full consensus sites (R or K present at positions −2 and −3 from the S or T) and partial consensus sites (R or K only present at either position −2 or position −3 from the S or T) that were conserved among human and mouse Gli2 and Gli3 and were located outside the DNA-binding zinc finger domain (Figure S1A). In addition to the full consensus sites (P1–6) described previously (Pan et al., 2009; Price and Kalderon, 1999; Wang et al., 2000), we identified 15 partial consensus sites (hereafter called Pa–o; Figures 1B and S1B). Myc-tagged fragments of Gli3 containing various subsets of these sites were tested as PKA substrates using an in vitro kinase assay. Four fragments containing sites P1–4, P5,6, Pc–g, and Pm–o could be phosphorylated by PKA (Figures 1C and 1D). Interestingly, both the P1–6 and the Pc–g clusters are located in regions of Gli2/3 that are strongly conserved among the *Drosophila*, *Xenopus*, and mouse proteins (Figure 1E).

PKA Target Sites P1–6 Regulate Gli3 Repressor and Activator Functions

We first analyzed the six sites in the P1–6 cluster, which had previously been identified as PKA targets (Riobó et al., 2006; Wang et al., 2000; Figure 2A). We decided to study P1–6 in the context of both Gli3 and Gli2, since Gli3 is the major repressor (Gli3R) and Gli2 the major activator (Gli2A) in most tissues. To understand the role of specific sites within the P1–6 cluster in regulating the GliR/GliA balance, we made nonphosphorylatable alanine mutants of P1–4 (P1–4A), P5 and P6 (P5,6A), or of the entire P1-6 cluster (P1–6A) in Gli2 and Gli3. Since Gli proteins fail to be regulated by Hh signaling when overproduced in cells (Humke et al., 2010), we sought to evaluate these Gli mutants under endogenous expression levels. To that end, we stably expressed hemagglutinin (HA)-tagged Gli2/3 (HA-Gli2/3) mutants in NIH/3T3 fibroblasts using the Flp-In system, in which an expression

construct is introduced as a single-copy insertion into a defined locus in the genome by Flp-mediated recombination (Torres et al., 2009; Zhou et al., 2010). The Flp-In system allowed us to rapidly generate stable cell lines expressing Gli protein variants at near-endogenous (Figure S2A) and roughly equal (Figure 2B) levels.

Starting with Gli3, we verified that a wild-type (WT) HA-Gli3 behaved like its endogenous counterpart. Indeed, HA-Gli3(WT) could be processed into a HA-GliR fragment when expressed using the Flp-In system (Figure 2B). Consistent with previous reports (Pan et al., 2006, 2009; Tempé et al., 2006; Wang and Li, 2006), mutation of sites P1–4 into alanine was sufficient to block Gli3R formation, as neither Gli3(P1–4A) nor Gli3(P1–6A) was converted into Gli3R. In contrast, Gli3(P5,6A) readily formed Gli3R in unstimulated cells (Figure 2B). Prior reports have implicated all six sites in the P1–6 cluster in GliR formation (Wang et al., 2000), but these studies were based on transient Gli3 overexpression and required stimulation with high doses of forskolin for prolonged periods of time to produce Gli3R. Using experimental conditions that faithfully reflect endogenous Gli3 processing in untreated cells, we find that sites P5 and P6 are not involved in the PKA-dependent truncation of Gli3 into a repressor fragment.

The formation of Hh-induced Gli3A can be experimentally followed by two biochemical events: activated Gli3 translocates into the nucleus and undergoes hyperphosphorylation, which appears as a shift in the apparent molecular weight of Gli proteins on SDS-PAGE gels (Humke et al., 2010). As we have previously described for endogenous Gli3, treatment of cells with the Smo agonist SAG led to the redistribution of HA-Gli3(WT) into the nuclear fraction; nuclear HA-Gli3 also showed the characteristic reduction in electrophoretic mobility indicative of hyperphosphorylation (Figure 2C, top panel, and Figure S2B). In contrast, when all six of the P1–6 sites were simultaneously mutated to alanines, Gli3 accumulated to high levels in the nucleus even in the absence of Hh signaling (Figure 2C, middle panel, and Figure S2B). Saturating concentrations of SAG did not further increase the nuclear accumulation of HA-Gli3(P1–6A), showing that the mutation of these six residues makes Gli3 unresponsive to upstream Hh signals. Alanine mutations only in sites P5 and P6 increased levels of Gli3 in the nucleus seen in the absence of signaling but did not result in maximal nuclear accumulation; HA-Gli3(P5,6A) still moved to the nucleus in response to SAG (Figure 2C, bottom panel, and Figure S2B).

To measure transcriptional activity of the Gli3 mutants, we transiently transfected constructs encoding each protein and measured the activation of an Hh-dependent firefly luciferase reporter gene (Sasaki et al., 1997). Consistent with prior characterization of Gli3 as a weak transcriptional activator (Sasaki et al., 1997), both HA-Gli3(WT) and HA-Gli3(P1–4A) failed to substantially increase Hh-dependent luciferase expression. On the other hand, HA-Gli3(P1–6A) could activate the reporter gene (Figure 2D), confirming the role of P5 and P6 in limiting the ability of Gli3 to activate transcription. Neither HA-Gli3(P1–4A) nor HA-Gli3(P1–6A) could be processed to Gli3R (Figure 2B), and so differences in their ability to activate transcription cannot be attributed differences in Gli3R levels. All six sites in the P1–6 cluster play a role in tuning Gli3 activity, since HA-Gli3(P5,6A) also demonstrated low levels of transcriptional activity, analogous to that of HA-Gli3(P1-4A) (Figure S2C).

These results suggest that Gli3 may be regulated by graded dephosphorylation. Loss of P1–4 phosphorylation blocks Gli3R repressor formation but is insufficient for the full activation of Gli3. The additional loss of P5,6 phosphorylation is required to achieve complete transformation of Gli3 into Gli3A.

Sites P1–6 Determine the Transcriptional Activity of Gli2

Since Gli2 is the major transcriptional activator of Hh target genes in most tissues, we made a similar series of mutations in the P1–6 sites of Gli2. While WT HA-Gli2 can activate the Hh reporter in transient overexpression assays (Figure 3A; Sasaki et al., 1999), the Gli2(P1–6A) mutant was significantly more active at all doses tested. The P1–4A and P5,6A mutants of Gli2 showed an intermediate capacity to activate the reporter. Mutation of either P5 or P6 individually in combination with P1–4 also increased activity of Gli2, suggesting that P5 and P6 may be partially redundant (Figure S2D). Conversely, mutation of both sites P5 and P6 to aspartate (P5,6D), a phospho-mimetic mutation, substantially reduced the activating potential of Gli2 (Figure S2D). These results are consistent with an inhibitory role of P1–6 phosphorylation in the activation of Gli2.

To examine Gli2 regulation under physiological expression levels, we turned to Flp-In stable lines carrying HA-tagged Gli2 mutants (Figure S2A). Similar to its effect on Gli3, the P1–6A mutation in HA-Gli2 caused constitutive Hh-independent accumulation in the nucleus, consistent with Gli2(P1–6A) being a fully active molecule (Figure 3B). In order to correlate nuclear accumulation with transcriptional activity, we measured the expression of endogenous *Gli1*, a Hh target gene commonly used as a metric for pathway activity, in these same stable cell lines. In the absence of Hh signaling, Gli1 levels were not elevated in the line expressing HA-Gli2(WT), confirming that this exogenous protein is properly regulated (Figure S2E). To account for differences in expression levels of the HA-Gli2 variants (Figure 3C), we compared their specific activities, calculated as the level of Gli1 induction divided by the protein level of the corresponding HA-Gli2 variant. The specific activities of the mutants fell along a gradient: the HA-Gli2(P1–4A) and HA-Gli2(P5,6A) mutants demonstrated ~3- to 4-fold higher specific activity and the HA-Gli2(P1–6A) mutant displayed ~13-fold higher specific activity compared to HA-Gli2(WT) (Figure 3C). The high level of Gli1 in cells carrying Gli2(P1–6A) was resistant to inhibition by two Smo antagonists, cyclopamine and SANT-1 (Figures 3D and S2F), demonstrating that the activity of this mutant protein was independent of Smo. Importantly, all the stable cell lines (which also contain endogenous Gli2) were able to produce equivalent levels of Gli1 when stimulated with SAG, showing that they did not differ in their intrinsic capacity to activate Hh targets (Figure 3C). Since the Flp-In lines also expressed endogenous Gli2, the *GLI1* induction in response to SAG (Figure 3C) could not be used to infer the Hh-responsiveness of the HA-Gli2 variants expressed in these lines.

To analyze the ability of upstream Hh signaling to regulate the HA-Gli2 mutants in our Flp-In cell lines, we selectively depleted endogenous Gli2 with a small interfering RNA (siRNA) directed against its 3′ UTR (Figures 3E and S2G). Under these conditions,

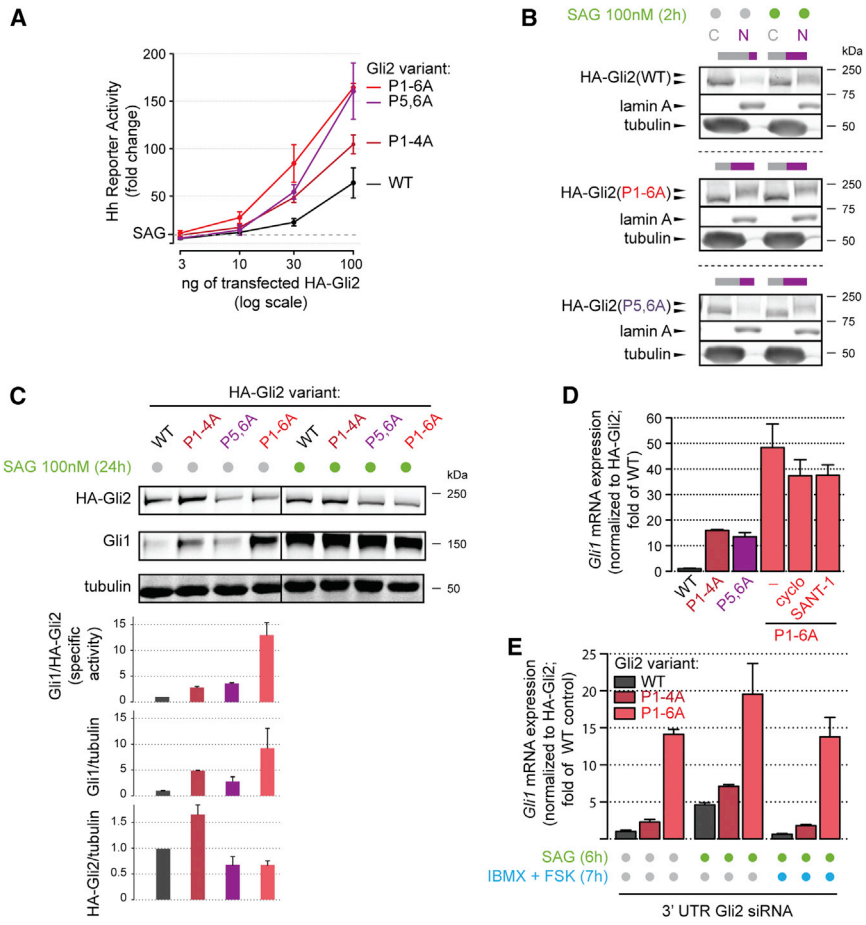

Figure 3. The P1–6 Cluster Regulates the Activation of Gli2

(A) Luciferase reporter activity in NIH/3T3 cells (untreated with any Hh agonists) transiently transfected with the indicated Gli2 variants. The dashed line shows levels of reporter induction seen when cells transfected with a control vector are exposed to SAG (100 nM). Error bars denote SD from three independent transfections.

(B) Distribution of full-length HA-Gli2 in NIH/3T3 Flp-In cells stably expressing the indicated variants.

(C) Levels of the Hh target gene Gli1 and HA-Gli2, measured using anti-Gli1 and anti-HA immunoblots respectively, in NIH/3T3 Flp-In stable cell lines expressing the indicated Gli2 variants. Cells were left untreated or treated with SAG (100 nM, 24 hr). Bar charts underneath show quantitation of the Gli1 and HA-Gli2 proteins (normalized to tubulin) in each cell line and the specific activity of each variant (top chart), expressed as the ratio of the intensities of the Gli1 band to the HA band. Bars denote the mean (±SD) from two independent experiments.

(D) *Gli1* mRNA level, measured by quantitative RT-PCR, in Flp-In stable cell lines expressing the indicated HA-Gli2 variants. HA-Gli2(P1-6A) cells were left untreated or treated with the Smo inhibitors cyclopamine (5 μM) or SANT-1 (100 nM). The *Gli1* mRNA level was normalized to the HA-Gli2 protein level as in (C) to adjust for differences in expression level of the Gli variants. Bars denote the mean (±SD) from two independent samples.

(E) *Gli1* mRNA level in the indicated stable cell lines treated with SAG (100 nM) in the presence or absence of the PKA activators IBMX (100 μM) and FSK (0.1 μM). In all cells, expression of endogenous Gli2 was reduced by a siRNA directed against the 3′ UTR to examine signaling through the HA-Gli2 variants. The *Gli1* mRNA level was normalized to HA-Gli2 protein measured as in (C) and (D); graphs depicting data without the HA-Gli2 protein normalization are shown in Figures S2F and S2G. Bars denote the mean (±SD) from two independent samples.

the SAG initiated signal should be largely transduced through our HA-tagged Gli2 variants. In the absence of endogenous Gli2, SAG could significantly increase *Gli1* expression in either HA-Gli2(WT) or HA-Gli2(P1–4A) cells. In the same cell lines, PKA activation, accomplished with the drugs isobutylmethylxanthine (IBMX) and forskolin (FSK) antagonized the effect of SAG (Figure 3E). In contrast, the high baseline expression of Gli1 in the HA-Gli2(P1–6A) line was largely insensitive to regulation by either SAG or IBMX/FSK (Figures 3E and S2G). This is further evidence that Gli2(P1–6A) corresponds to a maximally active form of Gli2, which cannot be regulated by either Smo or PKA. Gli2(P1–4A) remains SAG and PKA sensitive, perhaps through phosphoregulation at the P5 and P6 sites. We conclude that only after losing all phosphates at sites P1–6 does Gli2 become a bona fide GliA. These data explain why the previously studied Gli2(P1–4A) mutant of Gli2 failed to fully activate Hh responses during development (Pan et al., 2009).

P1–6 Mutants of Gli2 Ectopically Specify Ventral Cell Types in the Developing Spinal Cord

Encouraged by these results, we tested the ability of Gli2(P1–6A) to drive Hh-regulated cell fate decisions in vivo in a cell-autonomous manner. In the ventral neural tube, Shh acts as a graded signal that specifies the dorsal-ventral pattern of progenitor subtypes (Figure 4A). This precise spatial patterning is established by a gradient of Gli activity (Bai et al., 2004; Lei et al., 2004; Stamataki et al., 2005), making the neural tube an ideal place to test the activities of our Gli2(P1–4A) and Gli2(P1–6A) mutants. Using in ovo electroporation techniques, we expressed the Gli2 mutants under the control of a weak SV40 early promoter in one-half of the neural tube of Hamburger-Hamilton (HH) stage 10–12 chicken embryos and examined the expression of various progenitor markers 48 hr later. Ectopic expression of Gli2(WT) did not alter the spatial arrangement of neuronal progenitors (Figures 4B–4D, top row, and Figure S3C) and also did not induce expression of *PTCH1*, a direct Hh target gene (Figure 4E, top row).

In contrast, overexpression of Gli2(P1–6A) at any position along the dorsoventral axis led to the ectopic specification of ventral cells, identified by the ventral-most progenitor domain (pFP/p3) marker FOXA2 and the p3 marker NKX2.2, both of which depend on the highest levels of Hh/Gli signaling (Figure 4B, bottom row, and Figure S3C). Gli2(P1–6A) could also induce NKX6.1, which labels the pFP, p3, pMN, and p2 progenitor

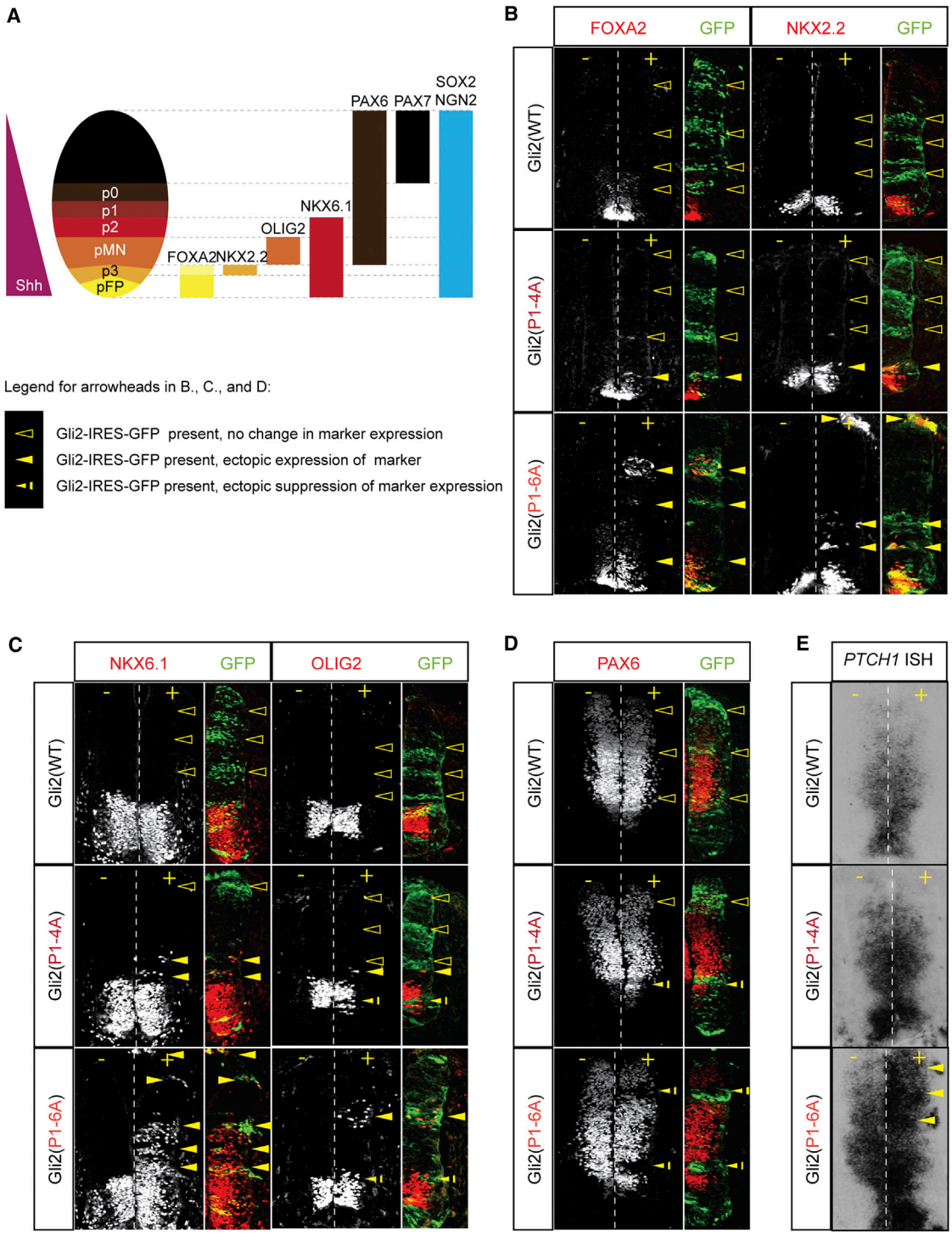

Figure 4. Gli2(P1-6A) Can Induce Ventral Cell Fates in the Developing Spinal Cord

(A) A schematic illustrating the relationship between marker proteins and progenitor cell populations in the embryonic neural tube (adapted from Stamataki et al., 2005). pFP, floor plate progenitors; pMN, motor neuron progenitors; p0, p1, p2, p3, ventral interneuron progenitors.

(B–D) Constructs encoding Gli2 variants (green) were electroporated into developing spinal cords of chicken embryos. Expression of the indicated progenitor population markers (red) was detected by immunofluorescence 48 hr later. Black and white panels show marker expression in both sides of the spinal cord ("+" indicates the electroporated side, "−" the unelectroporated side). Overlay panels show the electroporated side only. See also Figure S3C.

(E) In situ hybridization for *PTCH1* mRNA in sections of spinal cord electroporated with the indicated Gli2 constructs. The right side of each section was electroporated.

Cell PRESS
Open ACCESS

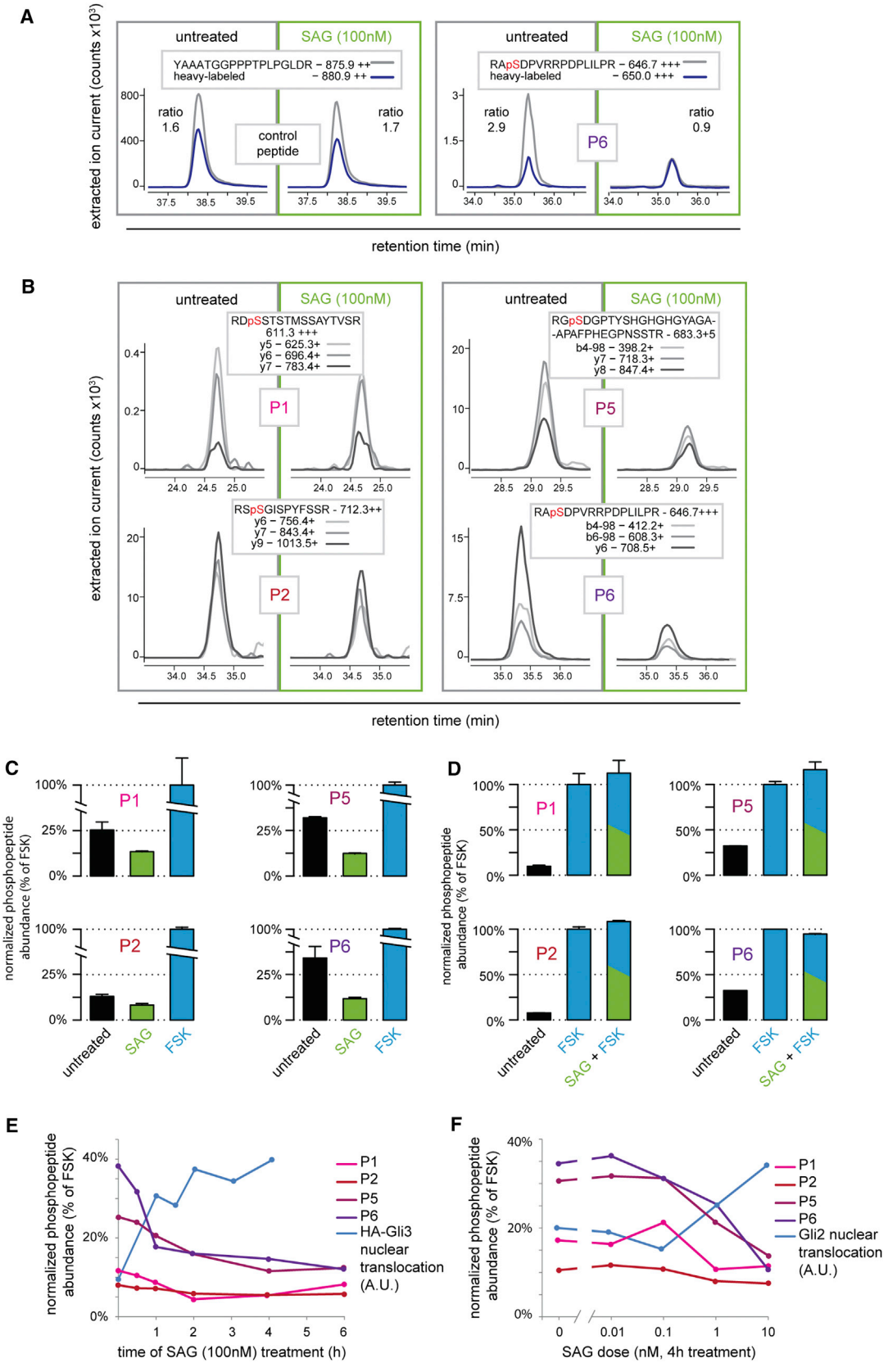

(legend on next page)

domains. OLIG2, a marker of motor neuron progenitors (pMN), which are specified by intermediate levels of Hh signaling, was induced mostly in cells expressing lower levels of Gli2(P1–6A) but often suppressed in strongly Gli2(P1–6A)-positive cells, most likely reflecting the cross-repressive interaction between NKX2.2 and OLIG2 in the neural tube (Novitch et al., 2001). Moreover, Gli2(P1–6A) suppressed the expression PAX6, a dorsal marker known to be negatively regulated by Hh signaling. Consistent with this ability to specify cell fates that depend on high levels of Hh ligand, Gli2(P1–6A) induced the robust expression of *PTCH1*, a direct Hh target gene, throughout the neural tube. The ability Gli2(P1–6A) to induce the ventral and suppress the dorsal markers was resistant to coexpression of a constitutively active mutant of Patched, $Ptch^{\Delta loop2}$ (Briscoe et al., 2001), confirming that the P1–6A mutant of Gli2 escapes regulation by the upstream elements of the Hh pathway (Figure S3A).

Gli2(P1–4A) demonstrated intermediate activity: it induced FOXA2, NKX2.2, and NKX6.1 when expressed immediately adjacent to their normal domains but not when expressed in more dorsal regions of the neural tube (Figures 4B–4D, middle row, and Figure S3C). This expansion of the ventral domains suggests that Gli2(P1–4A) sensitized cells to Shh, such that the same level of Shh exposure is translated to more ventral cell fates. Even though our Gli2 variants induced ectopic FOXA2, they did not drive SHH expression (Figure S3B), suggesting that the effects we describe in Figure 4 were not due to non-cell-autonomous effects of ectopic floor plate induction in the electroporated spinal cords. These data are consistent with previous reports showing that activated Smo and Gli proteins expressed in the HH12 stage neural tube can promote ventral character while at the same time inhibiting the formation of floor-plate cells (Lei et al., 2004; Ribes et al., 2010). Neither Gli2 mutant affected the expression of Hh-independent progenitor markers SOX2 and NGN2, suggesting that the total number of neuronal progenitors is unchanged by the expression of these constructs (Figure S3B).

Taken together, these data suggest that there is a fundamental difference between blocking phosphorylation at sites P1–4 only and blocking it throughout the P1–6 cluster. Because both the P1–4A and P1–6A mutations block repressor formation (Figure 2B), the marked differences in the activities of Gli2(P1–4A) and Gli2(P1–6A), both in cultured cells and in the developing neural tube, must be attributed to the role of P5 and P6 in the formation of Gli2A. Dephosphorylation of these sites in response to Hh ligands appears to be necessary to unleash the full activation potential of Gli2. P6 phosphorylation has been previously implicated in the interaction of Glis with 14-3-3 proteins (Asaoka et al., 2010), but in our system, this interaction did not appear to be required for the inhibitory function of P6 in GliA formation (see Supplemental Discussion and associated Figures S6B and S6C).

Hh Signaling Reduces Phosphorylation of P1–6

Our mutagenesis studies suggested that loss of phosphorylation on the serine residues at P1–6 is a regulatory step in the activation of Gli proteins. Hence, we sought to monitor changes in the phosphorylation status of these sites on endogenous Gli2 in response to signaling. We were unable to raise phospho-specific antibodies that recognized multiple sites on endogenous Gli2 in a quantitative fashion. Instead, we developed a mass spectrometry (MS)-based selected reaction monitoring (SRM) assay to quantitatively assess phosphate occupancy at P1, P2, P5, and P6 (Cox et al., 2005; Gerber et al., 2003; Mayya et al., 2006). Endogenous Gli2, isolated by immunoaffinity purification, was digested with trypsin, and the phosphorylated versions of the tryptic peptides encompassing sites P1, P2, P5, and P6 were quantified by triple-quadrupole MS (Figure 5A).

Activation of Hh signaling by SAG reduced the abundance of phosphorylated peptides containing sites P1, P2, P5, and P6 (Figures 5B and 5C), with changes at P5 and P6 being more marked than those in sites P1 and P2. The phosphorylation of sites P5 and P6 was sensitive to both the concentration of SAG and the duration of SAG treatment (Figures 5E and 5F). In both cases, reduction in phosphorylation correlated with the amount of Gli in the nucleus. The changes in Gli2 phosphorylation were not due to differences in protein stability, since all measurements were conducted on cells pretreated with the proteasome inhibitor bortezomib and results obtained in the absence and presence of this drug were similar (Figures 5C and S4A). In addition, no changes were observed after SAG addition in the abundance of a control, nonphosphorylatable peptide from a different region of Gli2 (Figure 5A). A caveat with measuring dephosphorylation by quantitative MS is that the observed reduction in the abundance of a phosphopeptide might reflect a change in phosphate occupancy of nearby sites rather than actual dephosphorylation of the site of interest. To address this concern, we also monitored the nonphosphorylated

Figure 5. Phosphorylation of the P1–6 Sites Declines with Hh Signaling

(A) Measurement of phosphopeptide abundance using SRM. Peptides were monitored in tryptic digests of immunoprecipitated Gli2 either in untreated NIH/3T3 Flp-In cells or in cells treated for 4 hr with 100 nM SAG, both in the presence of the proteasome inhibitor bortezomib (1 μM). The intensity of the "strongest" transition for two peptides, a nonphosphorylatable peptide used as a loading control (left) and a phospho-P6-containing peptide (right), was plotted versus retention time (XIC, extracted ion current; gray trace). Blue traces are XICs of the corresponding heavy isotope-labeled standard peptide spiked into the tryptic digest before the run. For each condition, the normalized abundance of a peptide was calculated as the ratio of the area under the curve (AUC) for the light (endogenous) peptide to the AUC for the heavy peptide.

(B) XIC versus retention time plots showing three SRM transitions for each of the endogenous (light) phosphorylated peptides containing sites P1, P2, P5, and P6.

(C and D) Normalized abundance of phosphopeptides (calculated using an SRM assays of the kind shown in A) containing the P1, P2, P5, and P6 sites derived from tryptic digests of immunopurified Gli2 isolated from NIH/3T3 cells treated (4 hr) with SAG (100 nM) or IBMX (100 μM) + FSK (100 nM). Phosphopeptide abundance measured in cells after PKA activation with IBMX + FSK was taken as maximal (100%) phosphorylation. Bars denote means (±SD) of two to three independent MS runs.

(E and F) Phosphopeptide abundance was monitored as a function of time after SAG treatment (E) and as a function of SAG concentration (F) and compared to the levels of Gli3 (E) or Gli2 (F) in the nucleus (blue line). Percent of total Gli in the nucleus was calculated based on subcellular fractionation experiments as shown in Figure 2C (Humke et al., 2010).

peptide encompassing site P6 (dephospho-P6) by SRM and observed that its abundance rose with SAG treatment and declined with IBMX and FSK (reciprocal to the pattern seen with phospho-P6; Figure S4B), suggesting that the changes in phospho-P6 were due to bona fide dephosphorylation of the P6 site.

Stimulation of PKA activity with IBMX and FSK strongly increased phosphate occupancy at all sites within the P1–6 cluster and also prevented SAG from decreasing phosphorylation (Figure 5D). This result is consistent with the model that PKA negatively regulates Hh signaling by phosphorylating P1–6. It also suggests that even in resting cells, Gli proteins are not fully phosphorylated at the P1–6 sites. The reason why these partially dephosphorylated Glis do not become transcriptionally active is unknown but may be related to the dynamics of the phosphate turnover on individual sites within the cluster. For instance, there may be some redundancy between individual sites in the P1–4 and P5,6 clusters.

A Cluster of Serine/Threonine Sites Is Important for Gli2/3 Activation

Since phosphorylation of the P1–6 cluster seemed sufficient for the inhibition of GliA formation, we were curious to determine how the two remaining clusters of putative PKA target sites (Pc–g, Pm–o; Figures 1B and 1C) affected Gli function. Alanine mutations in Pm–o cluster did not have a discernable effect (Figure S5A) in our assays, so we focused on the Pc–g cluster. To explore the role of Pc–g phosphorylation in the regulation of Gli2, we made both nonphosphorylatable and phosphomimetic mutations of this cluster in Gli2, replacing the serine and threonine residues with alanine or glutamate [hereafter called Gli2(Pc–gA) and Gli2(Pc–gE)]. In Hh reporter assays, HA-Gli2(Pc-gE) was significantly more active than the WT protein (Figure 6A) and Gli2(Pc–gA) was approximately 40% less active than the WT protein (Figure 6B). We also generated cell lines stably expressing HA-Gli2(Pc–gE) using the Flp-In system. Gli2(Pc–gE) protein levels were lower than Gli2 (WT), suggesting that the mutant protein was less stable (Figure S5B). The higher specific activity of HA-Gli2(Pc–gE) (Figure 6C) supported the model that Pc–g phosphorylation, in contrast to P1–6 phosphorylation, plays a positive role in Gli2 activity. Gli2(Pc–gE) also showed other hallmarks of activation, including reduced mobility on a gel and higher levels in the nucleus (Figure 6D).

Hh Signaling Promotes and PKA Antagonizes Phosphorylation on Pg

The characterization of Pc–g phosphorylation as playing a positive role in Gli activity was inconsistent with our initial identification of these sites as in vitro targets for PKA (Figure 1), a kinase that has an inhibitory effect on Hh signaling in vertebrates (Epstein et al., 1996; Humke et al., 2010; Tukachinsky et al., 2010; Tuson et al., 2011). To monitor Pc–g phosphorylation in the context of endogenous Gli2 in cells, we established an SRM assay to measure levels of a phosphorylated tryptic peptide that encompassed Pg, the only site in the Pc–g cluster whose phosphorylation could be easily monitored by MS (Table S1). Surprisingly, in cells treated with FSK and IBMX to activate PKA, Pg phosphorylation was reduced (Figure 6E), demonstrating that the Pg site is not a bona fide PKA target in cells. Instead, we observed a 5-fold increase in the abundance of phosphorylated Pg upon SAG treatment (Figure 6E), supporting the mutational data pointing to a positive role for Pc-g phosphorylation in Gli2 activity. As for P6, we also monitored the abundance of a nonphosphorylated tryptic peptide encompassing site Pg (dephospho-Pg; Figure S5C). As expected, dephospho-Pg abundance dropped with SAG treatment and increased with IBMX + FSK treatment, providing further evidence for the positive regulation of Pc–g phosphorylation by the Shh signal. Experiments performed in the presence and absence of a proteasome inhibitor gave qualitatively similar results (Figure S5D).

Interestingly, both the temporal dynamics and SAG dose-sensitivity of Pc–g phosphorylation (Figures 6F and 6G) mirrored those of P1–6 dephosphorylation (Figures 5E and 5F). PKA activation had opposite effects on the phosphorylation of the Pc–g and P1–6 clusters, suppressing the former while promoting the latter (Figures 6E and 5D). A parsimonious interpretation of these data is that PKA prevents Pc–g phosphorylation and Gli activation by directly phosphorylating the P1–6 sites.

To dissect the hierarchy between the Pc–gE and P1–6 sites, we combined activating (Pc–gE) and inhibitory (Pc–gA) mutations in the Pc–g sites with either inactivating (P5,6D) or activating (P1–6A) mutations in the P1–6 sites (Figure 6H). In Hh reporter assays, the activities of the Gli2(Pc–gE/P5,6D) and Gli2(Pc–gE/P1-6A) combination mutants were very similar, demonstrating that activating modifications at Pc–g make the phosphorylation status of P1–6 irrelevant. Controls confirmed that the isolated P5,6D mutation is much less active than the P1–6A mutant. Conversely, introduction of the inactivating Pc–gA mutation into Gli2(P1–6A) caused a substantial drop in its constitutive activity both in transient transfection assays (Figure 6I) and in a stable cell line (Figure 6J). These results support the model that Pc–g phosphorylation is an activating event gated by PKA-regulated phosphorylation of the P1–6 sites.

DISCUSSION

Distinct Phospho-codes for Gli Activator and Gli Repressor Regulation

We show here that phosphorylation of Gli proteins at six PKA target sites (P1–6) is a central determinant of their transcriptional activity, controlling the production of both repressor (GliR) and activator (GliA) forms. Our data are most consistent with a model involving ordered changes of phosphate occupancy at sites located in two distinct serine/threonine clusters (Figure 7A). In resting cells, PKA phosphorylates sites P1–6 on Gli2/3, triggering proteasomal processing into GliR and blocking conversion into GliA. When Hh binds to Ptc, Smo inhibits P1–6 phosphorylation, initiating a pathway that ultimately leads to the production of GliA: Gli proteins undergo phosphorylation at the Pc–g cluster, enter the nucleus, and are converted to unstable transcriptional activator proteins. We propose that the full transcriptional activation of Gli proteins requires the loss of phosphates at the P1–6 cluster followed by the gain of phosphates at the Pc–g cluster. The relative ordering of these two events is demonstrated by the fact that PKA activation enhances P1–6 phosphorylation and blocks Pc–g phosphorylation

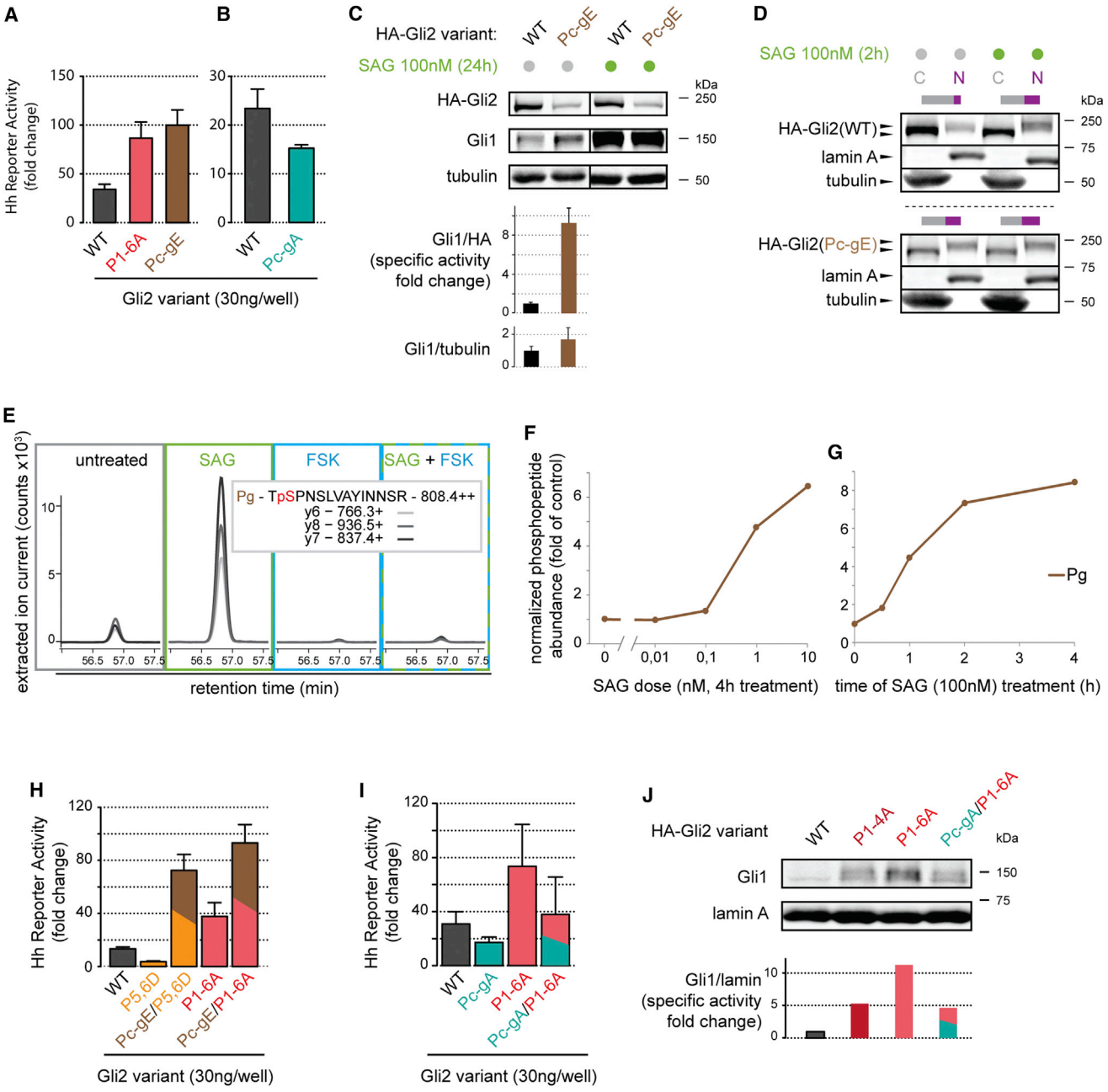

Figure 6. Pc–g Phosphorylation Positively Regulates Gli2 Activity

(A and B) Hh reporter activity in NIH/3T3 cells transiently transfected with Gli2(WT), Gli2(Pc-gA) or Gli2(Pc-gE). Bars are mean (±SD) of two independent transfections.

(C and D) NIH/3T3 Flp-In cell lines expressing HA-Gli2(WT) or HA-Gli2(Pc-gE) were used to evaluate the specific activity (C, analyzed as in Figure 3C) and subcellular distribution (D, analyzed as in Figure 2C) of the Gli2 variants. Bars are mean (±SD) of three independent experiments.

(E) XIC versus retention time traces for three SRM transitions derived from a Gli2 tryptic phosphopeptide containing the Pg residue. Phosphopeptide abundance is compared for Gli2 immunopurified from cells treated with the indicated drugs (4 hr).

(F and G) Pg phosphorylation abundance as a function of the concentration of SAG (F) or the duration of SAG exposure (G).

(H) Hh reporter activity in NIH/3T3 cells transiently transfected with Gli2(WT), Gli2(P5,6D), Gli2(P1–6A), and the combined mutants Gli2(Pc–gE/P1–6A) and Gli2(Pc–gE/P5,6D). Bars are mean (±SD) of three independent transfections.

(I) Hh reporter activity in NIH/3T3 cells transiently transfected with Gli2(WT), Gli2(Pc–gA), Gli2(P1–6A), and the combined mutant Gli2(Pc–gA/P1–6A). Bars denote mean ± SD from two independent transfections.

(J) Level of the Hh target gene Gli1 measured using anti-Gli1 immunoblot in cell lines stably expressing near-endogenous levels of the indicated HA-Gli2 constructs. Bar chart shows quantitation of Gli1 protein normalized to lamin.

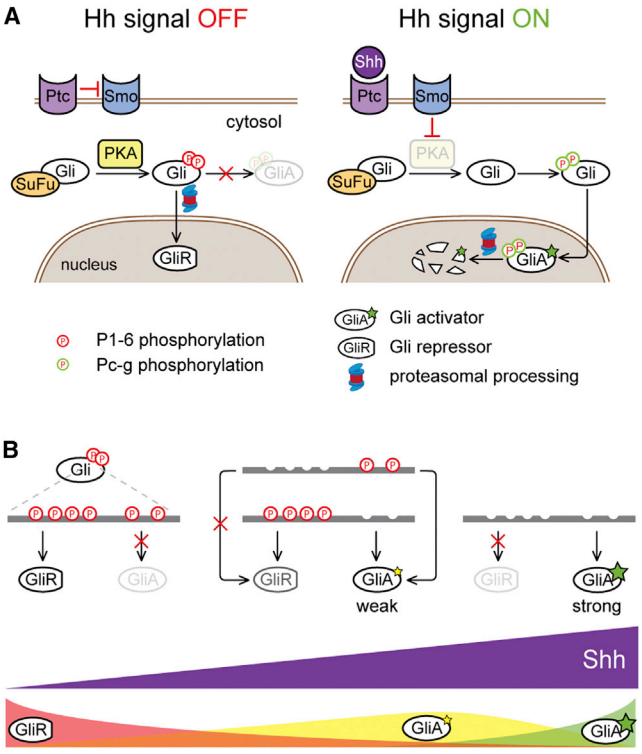

Figure 7. Our Model for the Phosphoregulation of Gli Proteins in Hh Signaling

(A) Diagram illustrating the multisite phosphorylation model of Gli2/3 regulation.

(B) Multiple states of Gli activity can be encoded by different patterns of Gli phosphorylation at the P1–6 cluster. Full phosphorylation of P1–6 (left) drives GliR formation and blocks GliA formation. Partially dephosphorylated Gli proteins (middle) function as weak activators and may be able to form GliR, depending on the pattern of phosphorylation. Fully dephosphorylated Gli proteins (right) cannot form GliR and function as strong transcriptional activators. See also Supplemental Discussion.

(Figure 6E). This regulatory motif, a gating dephosphorylation event coupled to nuclear translocation and an activating phosphorylation event at a distinct site, is reminiscent of the mechanism by which nuclear factor of activated T cells (NFAT) is regulated in response to T cell receptor engagement (Okamura et al., 2000). The concerted dephosphorylation of 13 phosphoserine residues by the phosphatase calcineurin triggers a conformational change in NFAT that drives nuclear localization. Like the Gli proteins, NFAT also requires an activating phosphorylation event at a separate site to acquire full transcriptional activity. Interestingly, in Gli1, which acts as a strong constitutive activator, the P1–6 cluster is poorly conserved (only sites P1, P2, and P6 show some degree of conservation). By contrast, four out of the five sites in the Pc–g cluster, including Pg, show remarkable sequence conservation among the three mammalian Gli proteins. This suggests that Pc–g phosphorylation may act as a universal activating signal for the Gli family.

Many signaling pathways, such as the NFAT pathway, regulate the conversion of a transcription factor from an inactive to an active state. The Hh pathway is different in that it controls the balance between gene repression, mediated by GliR, and gene activation, mediated by GliA. For instance, in *Drosophila*, low levels of Hh signaling suppress the formation of CiR, but higher levels are required for the production of CiA (Méthot and Basler, 1999, 2001). Our analysis of the P1–6 cluster in Gli3 (Figure 2) suggests that repressor and activator functions of Gli proteins can be encoded by different patterns of phosphorylation: loss of phosphates at P1–4 is enough to block repressor formation, but loss of phosphates at all six P1–6 residues is needed for full nuclear translocation and transcriptional activity (Figure 7B). This provides a simple mechanism by which signaling can exert independent control over the repressor and activator functions of Gli2/3.

While repressors forms of the Gli proteins can be assayed directly due to their truncated length, a reliable biochemical mark for Gli activator formation has remained elusive. GliA formation has been inferred indirectly from changes in subcellular localization, such as nuclear translocation, or from target gene activation. This is a clinically relevant issue, since such a mark of Gli protein activity would be a valuable predictive biomarker for patients being considered for Hh antagonists, and could be used as a pharmacodynamic parameter to assess responses. Our SRM MS analysis suggests that Pg phosphorylation can serve as such a marker for Gli2 activity.

Graded Control of Gli Activity by Multisite Phosphorylation

Why might Gli proteins be regulated through such a complex phosphorylation scheme? Multisite phosphorylation is a commonly used regulatory module in diverse signaling systems (reviewed in Salazar and Höfer, 2009). It can be used to engineer an ultrasensitive ON/OFF switch or to encode a rheostat, allowing graded responses to varying signal strength. Examples of the latter include graded enhancement of p53 binding to CREB in response to genotoxic stress (Lee et al., 2010), graded binding of Ets-1 to DNA (Pufall et al., 2005), and graded regulation of the gating properties of the Kv2.1 potassium channel (Park et al., 2006). In fact, a theoretical model has shown that multisite phosphorylation may serve to refine such a rheostat by allowing multistability, the existence of multiple discrete activity states in the target protein or signaling module (Thomson and Gunawardena, 2009). A multistable rheostat would be well adapted to the function that Gli proteins serve during embryonic development. In developmental fields such as the limb, the inner ear, and the neural tube, Hh ligands function as classical morphogens, and a central task of signaling is to translate ligand exposure into discrete outputs, such as cell fate, at the level of transcription (Bai et al., 2004; Bok et al., 2007; Fuccillo et al., 2004; Stamataki et al., 2005). Multisite phosphorylation might provide one mechanism by which differences in signal strength are converted into multiple discrete states of Gli activity (Figure 7B).

Indeed, our mutant analysis of the P1-6 cluster in Gli2 (Figures 3 and 4) is not consistent with a model in which Gli2 exists in either a fully inactive or fully active state. Particularly pertinent is the observation that both the P5,6A and the P1–4A mutants of Gli2 show an intermediate intrinsic capacity for transcriptional activation, which is higher than that of the WT protein but

significantly lower than that of the P1–6A mutant. Thus, Gli2 may occupy multiple states with differing activity, states that could represent different conformations of Gli2 that are stabilized by different patterns of phosphorylation at the P1–6 and Pc-g clusters. An important question going forward will be to ascertain how these changes in phosphate occupancy at the two conserved serine/threonine clusters affect the ability of Gli proteins to interact with other proteins in the cytoplasm, the cilium, and the nucleus and how these changes ultimately shape the Hh transcriptional program (also see Supplemental Discussion).

EXPERIMENTAL PROCEDURES

Cell Culture

293T cells, NIH/3T3 cells, and NIH/3T3 Flp-In cells (Life Technologies), including derivative stable clones, were cultured in media composed of Dulbecco's modified Eagle's medium (high glucose), 10% fetal bovine serum (FBS; Thermo Fisher Scientific), 1× GlutaMAX, 1× nonessential amino acids, 1× sodium pyruvate, and 1× penicillin/streptomycin (all from Life Technologies). Prior to harvesting, the cells were serum-starved in the same media but containing 0.5% FBS for 24–36 hr and treated with the indicated drugs/compounds. The 24 hr starvation was only used in assays where treatment time was 18–24 hr. For shorter treatment times (2–6 hr), a 36 hr starvation was preferred to induce a rapid response.

In Vitro Phosphorylation

Myc-tagged Gli2/3 fragments were cloned into pCS2 and overexpressed in HEK293T cells. In vitro phosphorylation was carried out on immunoprecipitated proteins in the PKA reaction buffer (Promega) in the presence of 0.5 mM ATP, 10 μCi of [γ-^{32}P]ATP, and 21 U of PKA (NEB) for 30 min at 30°C. See Supplemental Experimental Procedures for more details.

Hedgehog Reporter Luciferase Assay

The Hedgehog reporter luciferase assay was performed as described by us before (Dorn et al., 2012). See Supplemental Experimental Procedures for more details. All plots are mean ± SD.

Generation of Stable Cell Lines

Stable cell lines expressing low levels of HA-tagged Gli2 and Gli3 variants were generated using the Flp-In method exactly according to the manufacturer's recommendations (Life Technologies). Briefly, cells were cotransfected with pOG44 and the pEF5/FRT/V5-DEST vector containing the Gli2/3 construct of interest. After 2 days, the cells were reseeded at low density and the culture media was supplemented with hygromycin for stable integrant selection. Stable cell lines were reselected with hygromycin on every other passage to preserve selection pressure and prevent silencing of the transgene.

Subcellular Fractionation

The method for subcellular fractionation has been described by us in detail previously (Humke et al., 2010). Quantification of western blot bands was performed using ImageJ. Percent of the Gli2/3 variant present in the nuclear fractions was calculated for each sample by dividing the integrated band density for the nuclear fraction by the sum of densities for the cytoplasmic and nuclear fraction of the same sample.

In Ovo Electroporation and Immunohistochemistry/In Situ Hybridization of Chick tissue

HH stage 10–12 chick embryos were electroporated as previously described (Novitch et al., 2001) and incubated for ~48 hr to HH stages 20–22. See Supplemental Experimental Procedures for detailed methods of tissue staining and a list of reagents used.

Selected Reaction Monitoring Mass Spectrometry

Cells from two to six confluent 150 mm tissue culture dishes were serum-starved for 36 hr and treated for indicated times with SAG and/or IBMX + FSK. Bortezomib (1 μM) was added 4 hr prior to harvesting unless indicated otherwise. The cell lysate was collected under denaturing conditions and then diluted in RIPA buffer for immunoprecipitation. Endogenous Gli2 was immunoprecipitated and the eluted protein was resolved using SDS-PAGE. The gel fragment containing Gli2 was excised and trypsinized. Tryptic fragments were extracted from the gel, purified using Oasis μElution columns, and loaded onto a nano high-performance liquid chromatography system for separation and MS analysis (Abell et al., 2011). See Supplemental Experimental Procedures for more details regarding protein harvesting, purification, and SRM.

SUPPLEMENTAL INFORMATION

Supplemental Information includes Supplemental Discussion, Supplemental Experimental Procedures, six figures, and one table and can be found with this article online at http://dx.doi.org/10.1016/j.celrep.2013.12.003.

ACKNOWLEDGMENTS

We would like to thank Siggy Nachtergaele, Andres Lebensohn, and Ganesh Pusapati for critical reading of the manuscript, Casey Hughes for technical assistance, and James Briscoe for insightful discussions. This work was supported by NIH grants R21NS074091 and R00CA129174 (to R.R.), R01NS072804 and R01NS053976 (to B.G.N.), and P50GM107615 (to M.T.) and by grants from the V Foundation (to R.R.), the Sontag Foundation (to R.R.), the German Research Foundation (grant AH 220/1-1, to R.A.), and the March of Dimes Foundation (grant 6-FY10-296, to B.G.N.).

Received: September 30, 2013
Revised: November 7, 2013
Accepted: December 3, 2013
Published: December 26, 2013

REFERENCES

Abell, E., Ahrends, R., Bandara, S., Park, B.O., and Teruel, M.N. (2011). Parallel adaptive feedback enhances reliability of the Ca2+ signaling system. Proc. Natl. Acad. Sci. USA *108*, 14485–14490.

Asaoka, Y., Kanai, F., Ichimura, T., Tateishi, K., Tanaka, Y., Ohta, M., Seto, M., Tada, M., Ijichi, H., Ikenoue, T., et al. (2010). Identification of a suppressive mechanism for Hedgehog signaling through a novel interaction of Gli with 14-3-3. J. Biol. Chem. *285*, 4185–4194.

Bai, C.B., Stephen, D., and Joyner, A.L. (2004). All mouse ventral spinal cord patterning by hedgehog is Gli dependent and involves an activator function of Gli3. Dev. Cell *6*, 103–115.

Aza-Blanc, P., Ramírez-Weber, F.A., Laget, M.P., Schwartz, C., and Kornberg, T.B. (1997). Proteolysis that is inhibited by hedgehog targets Cubitus interruptus protein to the nucleus and converts it to a repressor. Cell *89*, 1043–1053.

Bok, J., Dolson, D.K., Hill, P., Rüther, U., Epstein, D.J., and Wu, D.K. (2007). Opposing gradients of Gli repressor and activators mediate Shh signaling along the dorsoventral axis of the inner ear. Development *134*, 1713–1722.

Briscoe, J., and Thérond, P.P. (2013). The mechanisms of Hedgehog signalling and its roles in development and disease. Nat. Rev. Mol. Cell Biol. *14*, 416–429.

Briscoe, J., Chen, Y., Jessell, T.M., and Struhl, G. (2001). A hedgehog-insensitive form of patched provides evidence for direct long-range morphogen activity of sonic hedgehog in the neural tube. Mol. Cell *7*, 1279–1291.

Corbit, K.C., Aanstad, P., Singla, V., Norman, A.R., Stainier, D.Y.R., and Reiter, J.F. (2005). Vertebrate Smoothened functions at the primary cilium. Nature *437*, 1018–1021.

Cox, D.M., Zhong, F., Du, M., Duchoslav, E., Sakuma, T., and McDermott, J.C. (2005). Multiple reaction monitoring as a method for identifying protein post-translational modifications. J. Biomol. Tech. *16*, 83–90.

Dorn, K.V., Hughes, C.E., and Rohatgi, R. (2012). A Smoothened-Evc2 complex transduces the Hedgehog signal at primary cilia. Dev. Cell *23*, 823–835.

Epstein, D.J., Marti, E., Scott, M.P., and McMahon, A.P. (1996). Antagonizing cAMP-dependent protein kinase A in the dorsal CNS activates a conserved Sonic hedgehog signaling pathway. Development *122*, 2885–2894.

Fan, C.M., Porter, J.A., Chiang, C., Chang, D.T., Beachy, P.A., and Tessier-Lavigne, M. (1995). Long-range sclerotome induction by sonic hedgehog: direct role of the amino-terminal cleavage product and modulation by the cyclic AMP signaling pathway. Cell *81*, 457–465.

Fuccillo, M., Rallu, M., McMahon, A.P., and Fishell, G. (2004). Temporal requirement for hedgehog signaling in ventral telencephalic patterning. Development *131*, 5031–5040.

Gerber, S.A., Rush, J., Stemman, O., Kirschner, M.W., and Gygi, S.P. (2003). Absolute quantification of proteins and phosphoproteins from cell lysates by tandem MS. Proc. Natl. Acad. Sci. USA *100*, 6940–6945.

Hahn, H., Wicking, C., Zaphiropoulous, P.G., Gailani, M.R., Shanley, S., Chidambaram, A., Vorechovsky, I., Holmberg, E., Unden, A.B., Gillies, S., et al. (1996). Mutations of the human homolog of Drosophila patched in the nevoid basal cell carcinoma syndrome. Cell *85*, 841–851.

Hammerschmidt, M., Bitgood, M.J., and McMahon, A.P. (1996). Protein kinase A is a common negative regulator of Hedgehog signaling in the vertebrate embryo. Genes Dev. *10*, 647–658.

Hill, P., Wang, B., and Rüther, U. (2007). The molecular basis of Pallister Hall associated polydactyly. Hum. Mol. Genet. *16*, 2089–2096.

Hui, C.-C., and Angers, S. (2011). Gli proteins in development and disease. Annu. Rev. Cell Dev. Biol. *27*, 513–537.

Humke, E.W., Dorn, K.V., Milenkovic, L., Scott, M.P., and Rohatgi, R. (2010). The output of Hedgehog signaling is controlled by the dynamic association between Suppressor of Fused and the Gli proteins. Genes Dev. *24*, 670–682.

Hynes, M., Porter, J.A., Chiang, C., Chang, D., Tessier-Lavigne, M., Beachy, P.A., and Rosenthal, A. (1995). Induction of midbrain dopaminergic neurons by Sonic hedgehog. Neuron *15*, 35–44.

Jiang, J., and Struhl, G. (1995). Protein kinase A and hedgehog signaling in Drosophila limb development. Cell *80*, 563–572.

Kang, S., Graham, J.M., Jr., Olney, A.H., and Biesecker, L.G. (1997). GLI3 frameshift mutations cause autosomal dominant Pallister-Hall syndrome. Nat. Genet. *15*, 266–268.

Kim, J., Kato, M., and Beachy, P.A. (2009). Gli2 trafficking links Hedgehog-dependent activation of Smoothened in the primary cilium to transcriptional activation in the nucleus. Proc. Natl. Acad. Sci. USA *106*, 21666–21671.

Lee, C.W., Ferreon, J.C., Ferreon, A.C.M., Arai, M., and Wright, P.E. (2010). Graded enhancement of p53 binding to CREB-binding protein (CBP) by multisite phosphorylation. Proc. Natl. Acad. Sci. USA *107*, 19290–19295.

Lei, Q., Zelman, A.K., Kuang, E., Li, S., and Matise, M.P. (2004). Transduction of graded Hedgehog signaling by a combination of Gli2 and Gli3 activator functions in the developing spinal cord. Development *131*, 3593–3604.

Lepage, T., Cohen, S.M., Diaz-Benjumea, F.J., and Parkhurst, S.M. (1995). Signal transduction by cAMP-dependent protein kinase A in Drosophila limb patterning. Nature *373*, 711–715.

Li, W., Ohlmeyer, J.T., Lane, M.E., and Kalderon, D. (1995). Function of protein kinase A in hedgehog signal transduction and Drosophila imaginal disc development. Cell *80*, 553–562.

Mayya, V., Rezual, K., Wu, L., Fong, M.B., and Han, D.K. (2006). Absolute quantification of multisite phosphorylation by selective reaction monitoring mass spectrometry: determination of inhibitory phosphorylation status of cyclin-dependent kinases. Mol. Cell. Proteomics *5*, 1146–1157.

Méthot, N., and Basler, K. (1999). Hedgehog controls limb development by regulating the activities of distinct transcriptional activator and repressor forms of Cubitus interruptus. Cell *96*, 819–831.

Méthot, N., and Basler, K. (2001). An absolute requirement for Cubitus interruptus in Hedgehog signaling. Development *128*, 733–742.

Niewiadomski, P., Zhujiang, A., Youssef, M., and Waschek, J.A. (2013). Interaction of PACAP with Sonic hedgehog reveals complex regulation of the hedgehog pathway by PKA. Cell. Signal. *25*, 2222–2230.

Novitch, B.G., Chen, A.I., and Jessell, T.M. (2001). Coordinate regulation of motor neuron subtype identity and pan-neuronal properties by the bHLH repressor Olig2. Neuron *31*, 773–789.

Okamura, H., Aramburu, J., García-Rodríguez, C., Viola, J.P., Raghavan, A., Tahiliani, M., Zhang, X., Qin, J., Hogan, P.G., and Rao, A. (2000). Concerted dephosphorylation of the transcription factor NFAT1 induces a conformational switch that regulates transcriptional activity. Mol. Cell *6*, 539–550.

Pan, D., and Rubin, G.M. (1995). cAMP-dependent protein kinase and hedgehog act antagonistically in regulating decapentaplegic transcription in Drosophila imaginal discs. Cell *80*, 543–552.

Pan, Y., Bai, C.B., Joyner, A.L., and Wang, B. (2006). Sonic hedgehog signaling regulates Gli2 transcriptional activity by suppressing its processing and degradation. Mol. Cell. Biol. *26*, 3365–3377.

Pan, Y., Wang, C., and Wang, B. (2009). Phosphorylation of Gli2 by protein kinase A is required for Gli2 processing and degradation and the Sonic Hedgehog-regulated mouse development. Dev. Biol. *326*, 177–189.

Park, K.-S., Mohapatra, D.P., Misonou, H., and Trimmer, J.S. (2006). Graded regulation of the Kv2.1 potassium channel by variable phosphorylation. Science *313*, 976–979.

Price, M.A., and Kalderon, D. (1999). Proteolysis of cubitus interruptus in Drosophila requires phosphorylation by protein kinase A. Development *126*, 4331–4339.

Pufall, M.A., Lee, G.M., Nelson, M.L., Kang, H.-S., Velyvis, A., Kay, L.E., McIntosh, L.P., and Graves, B.J. (2005). Variable control of Ets-1 DNA binding by multiple phosphates in an unstructured region. Science *309*, 142–145.

Ribes, V., Balaskas, N., Sasai, N., Cruz, C., Dessaud, E., Cayuso, J., Tozer, S., Yang, L.L., Novitch, B., Marti, E., and Briscoe, J. (2010). Distinct Sonic Hedgehog signaling dynamics specify floor plate and ventral neuronal progenitors in the vertebrate neural tube. Genes Dev. *24*, 1186–1200.

Riobó, N.A., Lu, K., Ai, X., Haines, G.M., and Emerson, C.P., Jr. (2006). Phosphoinositide 3-kinase and Akt are essential for Sonic Hedgehog signaling. Proc. Natl. Acad. Sci. USA *103*, 4505–4510.

Salazar, C., and Höfer, T. (2009). Multisite protein phosphorylation—from molecular mechanisms to kinetic models. FEBS J. *276*, 3177–3198.

Sasaki, H., Hui, C., Nakafuku, M., and Kondoh, H. (1997). A binding site for Gli proteins is essential for HNF-3beta floor plate enhancer activity in transgenics and can respond to Shh in vitro. Development *124*, 1313–1322.

Sasaki, H., Nishizaki, Y., Hui, C., Nakafuku, M., and Kondoh, H. (1999). Regulation of Gli2 and Gli3 activities by an amino-terminal repression domain: implication of Gli2 and Gli3 as primary mediators of Shh signaling. Development *126*, 3915–3924.

Stamataki, D., Ulloa, F., Tsoni, S.V., Mynett, A., and Briscoe, J. (2005). A gradient of Gli activity mediates graded Sonic Hedgehog signaling in the neural tube. Genes Dev. *19*, 626–641.

Strutt, D.I., Wiersdorff, V., and Mlodzik, M. (1995). Regulation of furrow progression in the Drosophila eye by cAMP-dependent protein kinase A. Nature *373*, 705–709.

Tempé, D., Casas, M., Karaz, S., Blanchet-Tournier, M.-F., and Concordet, J.-P. (2006). Multisite protein kinase A and glycogen synthase kinase 3beta phosphorylation leads to Gli3 ubiquitination by SCFbetaTrCP. Mol. Cell. Biol. *26*, 4316–4326.

Thomson, M., and Gunawardena, J. (2009). Unlimited multistability in multisite phosphorylation systems. Nature *460*, 274–277.

Torres, J.Z., Miller, J.J., and Jackson, P.K. (2009). High-throughput generation of tagged stable cell lines for proteomic analysis. Proteomics *9*, 2888–2891.

Tukachinsky, H., Lopez, L.V., and Salic, A. (2010). A mechanism for vertebrate Hedgehog signaling: recruitment to cilia and dissociation of SuFu-Gli protein complexes. J. Cell Biol. *191*, 415–428.

Tuson, M., He, M., and Anderson, K.V. (2011). Protein kinase A acts at the basal body of the primary cilium to prevent Gli2 activation and ventralization of the mouse neural tube. Development *138*, 4921–4930.

Wang, B., and Li, Y. (2006). Evidence for the direct involvement of betaTrCP in Gli3 protein processing. Proc. Natl. Acad. Sci. USA *103*, 33–38.

Wang, G., Wang, B., and Jiang, J. (1999). Protein kinase A antagonizes Hedgehog signaling by regulating both the activator and repressor forms of Cubitus interruptus. Genes Dev. *13*, 2828–2837.

Wang, B., Fallon, J.F., and Beachy, P.A. (2000). Hedgehog-regulated processing of Gli3 produces an anterior/posterior repressor gradient in the developing vertebrate limb. Cell *100*, 423–434.

Wen, X., Lai, C.K., Evangelista, M., Hongo, J.-A., de Sauvage, F.J., and Scales, S.J. (2010). Kinetics of hedgehog-dependent full-length Gli3 accumulation in primary cilia and subsequent degradation. Mol. Cell. Biol. *30*, 1910–1922.

Zhou, C., Jacobsen, F.W., Cai, L., Chen, Q., and Shen, W.D. (2010). Development of a novel mammalian cell surface antibody display platform. MAbs *2*, 508–518.